MR of Toxic Effects of Accelerated Fractionation Radiation Therapy and Carboplatin Chemotherapy for Malignant Gliomas

Pamela Van Tassel, Janet M. Bruner, Moshe H. Maor, Norman E. Leeds, Mary J. Gleason, W. K. Alfred Yung, and Victor A. Levin

PURPOSE: To present MR findings of parenchymal brain injury after accelerated fractionation radiation therapy combined with carboplatin chemotherapy in the treatment of malignant brain gliomas. **METHODS:** Eighty-one evaluable subjects in an ongoing treatment protocol for malignant gliomas form the patient base for this report. After surgical resection of tumors, patients underwent a course of accelerated fractionation radiation therapy to a total dose of 60 Gy. Carboplatin was infused intravenously before each radiation treatment. Precontrast and postcontrast MR scans were obtained before treatment and at 4-week intervals afterward and were analyzed retrospectively. **RESULTS:** Posttreatment MR imaging in 20 of the 81 patients showed development of unusual parenchymal lesions or enlarging masses needing debulking, and these patients underwent second operations. Two groups emerged: those with tumor and necrotic brain (n = 11) and those with necrosis and reactive gliosis but no definitive tumor (n = 9). Enhancing lesions in the tumor-negative group appeared later than those in the tumor-positive group, were often multiple, and were usually located several centimeters away from the tumor resection site or even contralaterally. Common locations were the corpus callosum and corticomedullary junctions. Lesions in the tumor-positive group were more often solitary and located immediately adjacent to the surgical site. Positive and negative results of positron emission tomography with fludeoxyglucose F 18 were obtained in both groups. The incidence of brain necrosis without associated tumor was 11%. **CONCLUSIONS:** A pattern of unusual enhancing parenchymal brain lesions was seen on MR imaging after accelerated fractionation radiation therapy and concomitant carboplatin chemotherapy. The abnormalities seem more extensive than focal necrotic lesions on enhanced CT or MR imaging after conventional radiation therapy, and they may mimic recurrent tumor.

Index terms: Brain, necrosis; Brain neoplasms, magnetic resonance; Radiation, injuries; Therapeutic radiology, complications; Iatrogenic disease or disorder

AJNR Am J Neuroradiol 16:715–726, April 1995

The grim prognosis of malignant gliomas has prompted trials of various chemotherapy and radiation therapy regimens in the hope of reducing the morbidity and mortality associated with these tumors. Surgical debulking, when possible, and conventionally fractionated radiation therapy are the most common treatments for these tumors (1, 2). Platinum-derivative drugs have shown efficacy in the treatment of primary brain tumors, particularly with respect to a synergistic effect when given during radiation therapy treatments (3, 4). At our institution, a treatment protocol was begun using simultaneous intravenous carboplatin during radiation therapy. The radiation therapy was delivered using accelerated fractionation to avoid reaching bone marrow toxicity from the carboplatin before the end of the radiation treatments. We report the incidence and magnetic resonance (MR) patterns of parenchymal brain injury encountered with this therapy and some distin-

Received July 27, 1994; accepted after revision November 10.

Presented at the 30th Annual Meeting of the American Society of Neuroradiology, St Louis, Mo, June 1992.

From the Departments of Radiology (P.V.T., N.E.L.), Pathology (J.M.B.), Radiation Oncology (M.H.M.), and Neurooncology (M.J.G., W.K.A.Y., V.A.L.), M.D. Anderson Cancer Center, Houston, Tex.

Address reprint requests to Pamela Van Tassel, MD, Department of Radiology, Medical University of South Carolina, 171 Ashley Ave, Charleston, SC 29425-2266.

AJNR 16:715–726, Apr 1995 0195-6108/95/1604–0715

guishing features compared with previous imaging descriptions of injury after standard fractionation radiation therapy.

Subjects and Methods

In 1988, patient enrollment commenced for a new treatment protocol for malignant gliomas at our institution, consisting of accelerated fractionation radiation therapy and concurrent carboplatin chemotherapy. The first 81 evaluable patients completing treatment form the basis of this report. The tumor types include 48 glioblastoma multiformes, 21 anaplastic astrocytomas, 6 anaplastic oligodendrogliomas, and 6 anaplastic mixed gliomas. The protocol is now closed to glioblastoma multiforme, because enough patients with this diagnosis for statistical validity have been accrued; patients with the other tissue types are still being enrolled.

After as complete a surgical resection as possible, a daily radiation dose of 600 cGy was given in three fractions of 200 cGy each for 5 consecutive days using a 6 MV linear accelerator. There was an interval of 4 hours between fractions. The portals included a 3-cm margin around the tumor. After a 2-week break, a second identical course was given for a total dose of 60 Gy in 10 days. Carboplatin at a dose of 33 mg/m^2 was given intravenously three times daily immediately before the radiation treatments. Additional intravenous chemotherapy consisting of procarbazine, lomustine, and vincristine was begun 4 weeks after radiation therapy and carboplatin ended and was repeated at 6-week intervals for 1 year or until tumor progression.

Twenty of the 81 patients underwent additional surgery for new enhancing parenchymal brain lesions, which appeared months to years after completion of radiation therapy (Table 1). Patients were operated on again to obtain a gross total resection of presumed recurrent tumor, to relieve mass effect produced by the abnormality, or to determine the cause of perplexing, unusual lesions. The majority of the 61 patients not receiving additional surgery had imaging findings suggesting rapid regrowth of tumor and a poorer neurologic performance status, and further intervention was not thought beneficial. In the group that underwent additional surgery, tissue was obtained by a stereotactic approach in 5 and by open resection in 15 patients. Autopsies were performed in 6 of the 20 patients.

Most patients had preoperative imaging studies performed at outside institutions, and the majority of these were MR scans performed on a variety of imagers. Most patients received follow-up imaging at our institution, using a 1.5-T magnet, and these were obtained within 1 month of surgery and at 4- to 6-week intervals thereafter. T1-weighted spin-echo (600/25/2 [repetition time/echo time/excitations]) scanning was performed in a least one plane before contrast administration. Precontrast T2-weighted (2000/20,80/1) images were also obtained. Gadopentetate dimeglumine was given intravenously in all patients at a dose of 0.1 mmol/kg, followed by T1-weighted imaging in the axial plane and supplemental coronal and sagittal views as needed. One of the 20 patients had precontrast and postcontrast computed tomography (CT) and not MR imaging. These studies were retrospectively reviewed by two senior members of the American Society of Neuroradiology (P.V.T. and N.E.L.), who were not blinded to histologic results and patient outcomes.

Positron emission tomography with fludeoxyglucose F 18 (FDG PET) was available for correlation in 10 of the 20 reoperated patients. After intravenous injection of 5 to 10 mCi of fludeoxyglucose F 18, three sets of axial images of the head were acquired.

TABLE 1: Patients with second surgery

Tumor Type	Tumor-Negative Group, n	Tumor-Positive Group, n
Glioblastoma multiforme	4	5
Anaplastic astrocytoma	2	3
Anaplastic mixed glioma	3	2
Anaplastic oligodendroglioma	0	0
Total	**9**	**11**

Results

Pathologic specimens from the 20 patients undergoing surgery after completing the combined accelerated radiation therapy and chemotherapy divided these patients essentially into two groups: those with necrosis, reactive or atypical gliosis, and no definitive tumor (n = 9), and those with necrosis, gliosis, and obvious tumor (n = 11).

Tumor-Negative Group (Table 2)

Within this group there was an average interval of 10 months from the end of therapy to the discovery of a new enhancing parenchymal abnormality (range, 5 to 13 months). All lesions were within the treatment portals. Patients with purely necrotic lesions tended to remain asymptomatic longer than those with recurrent malignant glioma as well as necrosis. Lesions were initially solitary on posttreatment scans in five and multiple in four of the nine patients. Three of those with solitary lesions later developed additional lesions. In seven patients the abnormalities were small, uniformly enhancing nodules; however, in six of these, the nodules became ring enhancing on subsequent scans. Two patients had heterogeneously enhancing lesions when first detected. Most lesions in each patient demonstrated progressive enlargement on follow-up scans. Two patients had at least one lesion that regressed while other lesions

TABLE 2: MR characteristics of new lesions

	Tumor-Negative Group (n=9)		Tumor-Positive Group (n=11)	
Time to new lesion	10 mo (range, 5–13 mo)		5 mo (range, <1–12 mo)	
Lesion(s) within radiation portal?	Yes	9	Yes	11
	No	0	No	1
Lesion multiplicity	Solitary	2	Solitary	7
	Multiple	7	Multiple	4
Lesion location	Corpus callosum/periventricular	7	White matter	8
	Corticomedullary	5	Corticomedullary	3
	White matter	4	Basal ganglion	1
Proximity of lesion(s) to original tumor	Edge of treated tumor	5	Within/at edge of treated tumor	11
	Several cm away, ipsilateral	8	Several cm away, ipsilateral	2
	Contralateral	7	Contralateral multicentric tumor	1
Enhancement pattern	Solid only	1	Solid only	3
	Solid progressing to ring enhancement	6	Solid progressing to heterogeneous	4
	Mixed solid and ring enhancement	2	Heterogeneous	4
Positron emission tomography correlation	Negative	4	Negative	3
	Positive	1	Positive	2

Note.—Numbers indicate numbers of patients with that characteristic.

remained stable or enlarged. Seven patients exhibited lesions in the corpus callosum or subependymal regions; five had lesions at corticomedullary junctions; and in four there were lesions epicentered in white matter. Five of the nine patients had a new lesion at the edge of the treated tumor; in eight patients, lesions were several centimeters away from the primary treatment site and ipsilateral. Seven patients had lesions contralateral to the site of the original tumor (Fig 1). FDG PET scanning was performed in five of the nine patients and was negative for a hypermetabolic lesion in four; in the fifth patient, one of numerous enhancing lesions was hypermetabolic.

Four of the patients in this group underwent stereotactic biopsies, and five underwent open resection of tissue. Tissue specimens from the tumor-negative group typically showed reactive gliosis, focal areas of necrosis, subendothelial hyalinization, and occasional calcifications. Variable numbers of gemistocytic astrocytes were often present, some with enlarged, atypical nuclei, but not exhibiting mitotic activity. This atypia at times made distinction between a low-grade tumor and reactive gliosis difficult.

There were three deaths in this group, and two autopsies were performed. In one of these patients, whose original tumor was a left frontal glioblastoma multiforme, periventricular nodular enhancing lesions appeared in the left corpus callosum 11 months after completion of treatment (Fig 2). FDG PET revealed no evidence of a hypermetabolic lesion. At 21 months, shortly before death, there was encasement of both lateral ventricles by a diffuse, enhancing process. Autopsy revealed extensive necrosis and reactive gliosis in the corpus callosum, the fornix, and the cerebral white matter. No definitive residual tumor could be found. The other autopsied patient seemed originally to have a bilateral multicentric tumor in the right parietal and left temporal lobes (Fig 3). Near-complete resection of the right-sided lesion was done, revealing anaplastic astrocytoma. The 60-Gy accelerated fractionation therapy was given to the whole brain. Small enhancing nodules appeared in the left frontal white matter and the brain stem 13 months after therapy. At 17 months after therapy, there were multiple solid and ring-enhancing periventricular and callosal lesions associated with the temporal horns and bodies of the lateral ventricles bilaterally. These progressively enlarged and showed more of a ring-enhancing pattern on subsequent scans. An FDG PET scan at 22 months after treatment showed hypermetabolic activity near the right temporal horn but not elsewhere. The patient died 35 months after treatment; autopsy showed extensive necrosis, gliosis, vascular hyalinization, and calcification affecting the corpus callosum, the fornix, the brain stem, the cerebral cortex, and the white matter of the cerebral hemispheres and

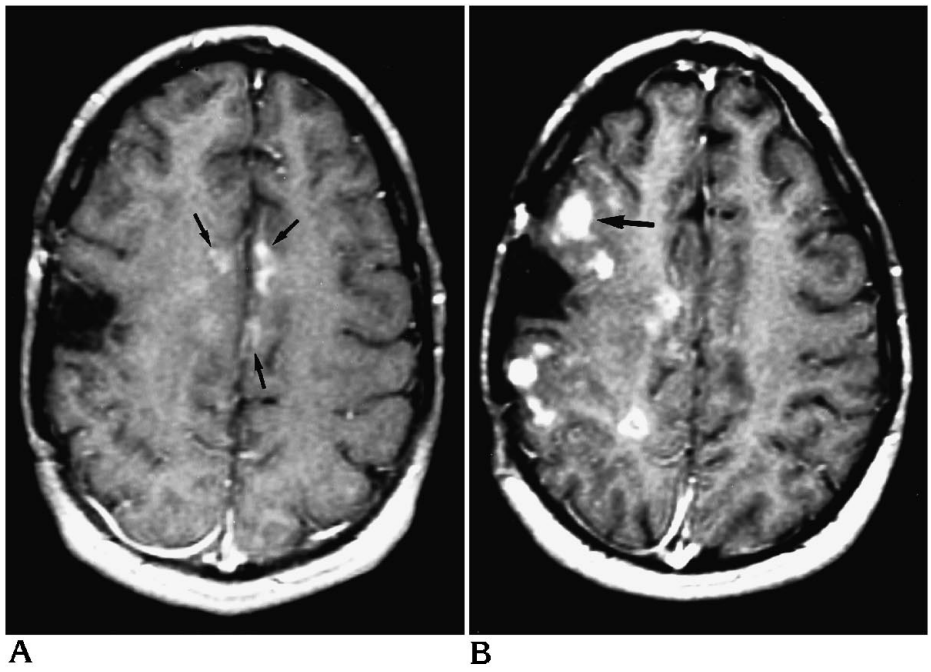

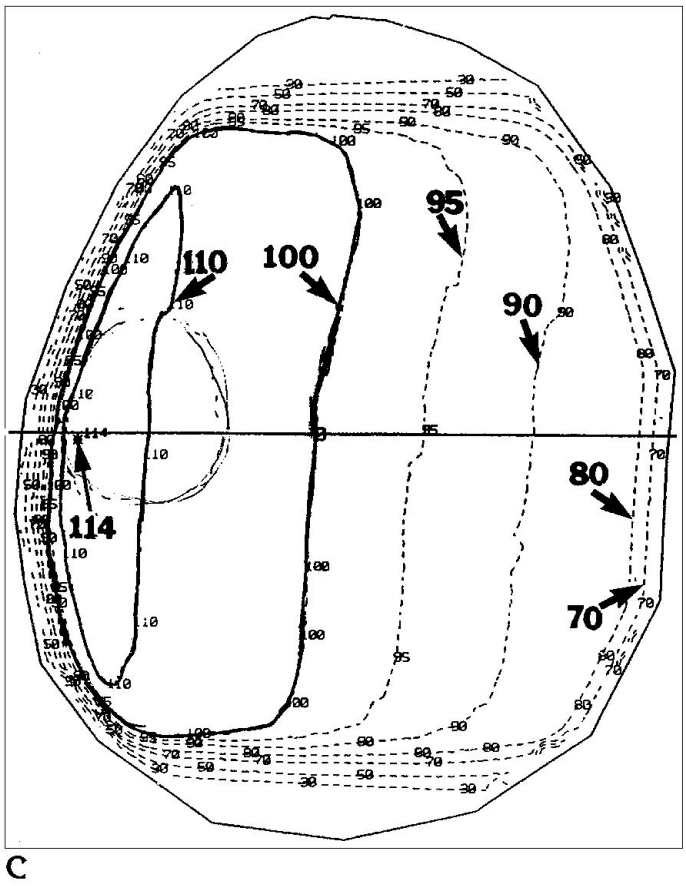

Fig 1. Patient from the tumor-negative group.

A, Postcontrast T1-weighted axial image 16 months after treatment for anaplastic astrocytoma shows a surgical defect laterally in the right anterior parietal lobe with no associated enhancement. (The original tumor was nonenhancing.) Abnormal enhancement is seen at parasagittal corticomedullary junctions bilaterally (*arrows*).

B, Axial postcontrast image 1 year after *A* demonstrates waning of the left frontoparietal lesions but new corticomedullary lesions near the original tumor site. Resection of the lesion marked by the *arrow* revealed necrosis, gliosis, and no tumor.

C, Radiation therapy isodose curves, numbers in percent. Lesions in *B* are located in the areas of highest dose.

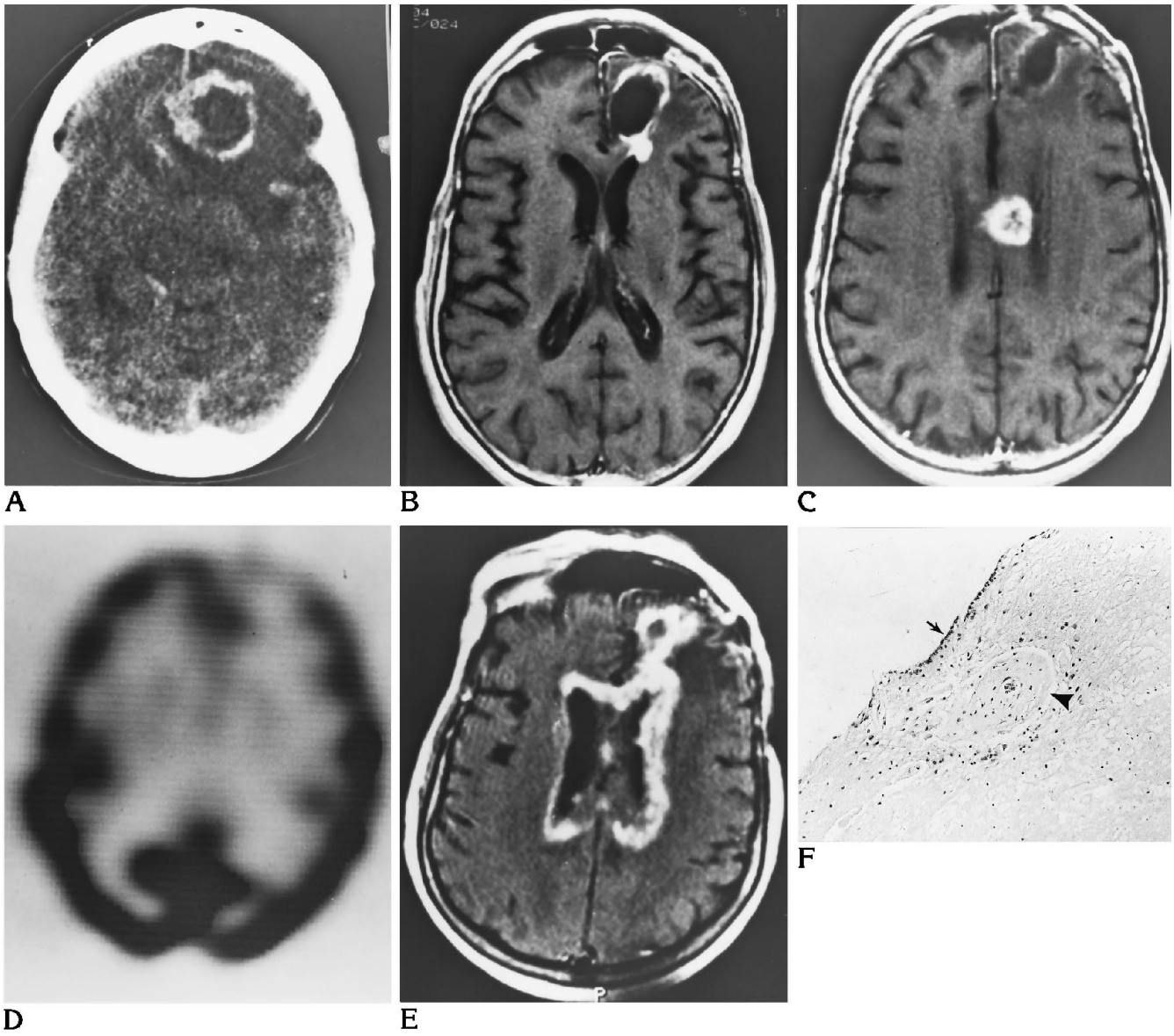

Fig 2. Patient from the tumor-negative group.

A, Preoperative postcontrast CT of a ring-enhancing left frontal glioblastoma.

B and *C*, Postcontrast images 11 months after surgery and radiation therapy show enhancement around the surgical cavity, especially posteriorly, and a separate lesion in the corpus callosum. A biopsy of the callosal lesion revealed only necrosis.

D, FDG PET scan 12 months after treatment, at approximately the same level as *C*. No hypermetabolic focus seen at the midline or in the left frontal lobe. There is decreased metabolism in the left frontal cortex.

E, Postcontrast scan 20 months after treatment shows extensive enhancement around the lateral ventricles and in the corpus callosum. Left frontal enhancement has also progressed.

F, Histopathologic section from the autopsied brain at the level of the lateral ventricle. The *arrow* indicates the ependymal surface; the *arrowhead*, vascular wall hyalinization. The normal neuropil is replaced by extensive necrosis. Hematoxylin and eosin, original magnification × 125.

the cerebellum. There were small foci of atypical astrocytes at the original surgical site in the right parietal lobe and also in the left medial occipital lobe, but no definitive tumor was found, particularly with reference to the positive right temporal lobe lesion on FDG PET.

Tumor-Positive Group (Table 2)

The patients in this group had an average time of 5 months between the conclusion of therapy and development a new enhancing abnormality (range, <1 to 12 months). Lesions in

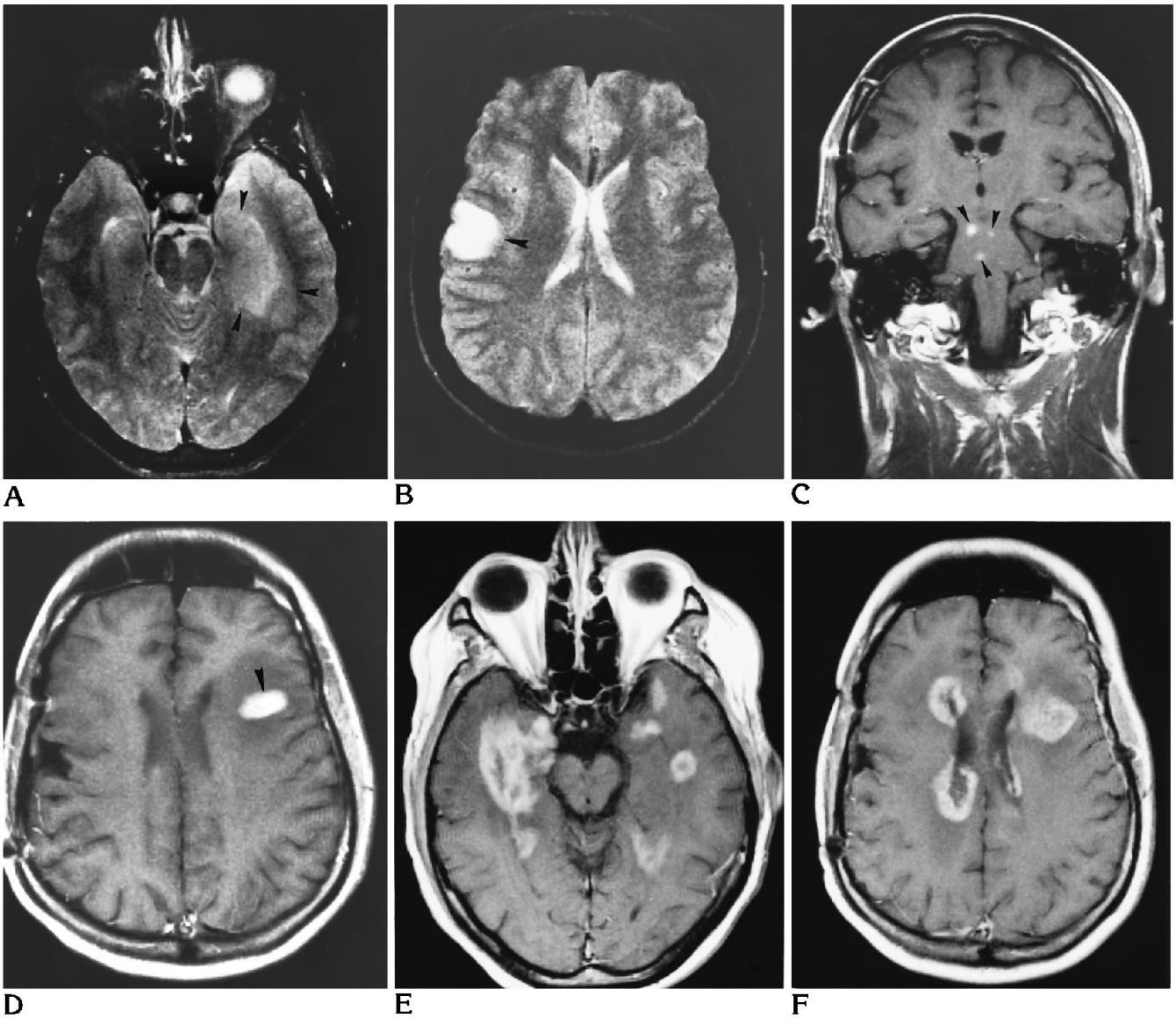

Fig 3. Patient in the tumor-negative group.

A and *B*, T2-weighted axial pretreatment scans showing multicentric lesions in the left medial temporal (*arrowheads*) and right anterior parietal lobes (pre–gadolinium-era scan).

C and *D*, Coronal and axial postcontrast images, 36 and 41 months, respectively, after *A* and *B*. These show a surgical defect laterally in the right cerebral hemisphere (anaplastic astrocytoma), no enhancement there or in left temporal lobe, and enhancing lesions in the pons and the left frontal lobe (*arrowheads*). A biopsy of the left frontal lesion revealed necrosis only.

E and *F*, Axial postcontrast images at 51 months show multiple ring-enhancing periventricular masses.

G, FDG PET image at same time as *E* and *F* demonstrates increased uptake in the right temporal lobe (*arrowhead*) but not elsewhere. At autopsy no definitive tumor was found here or in the other enhancing areas.

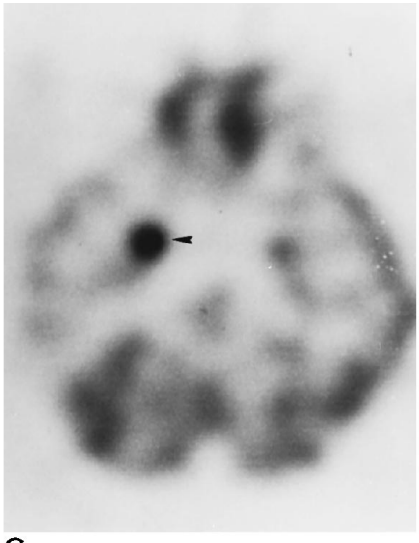

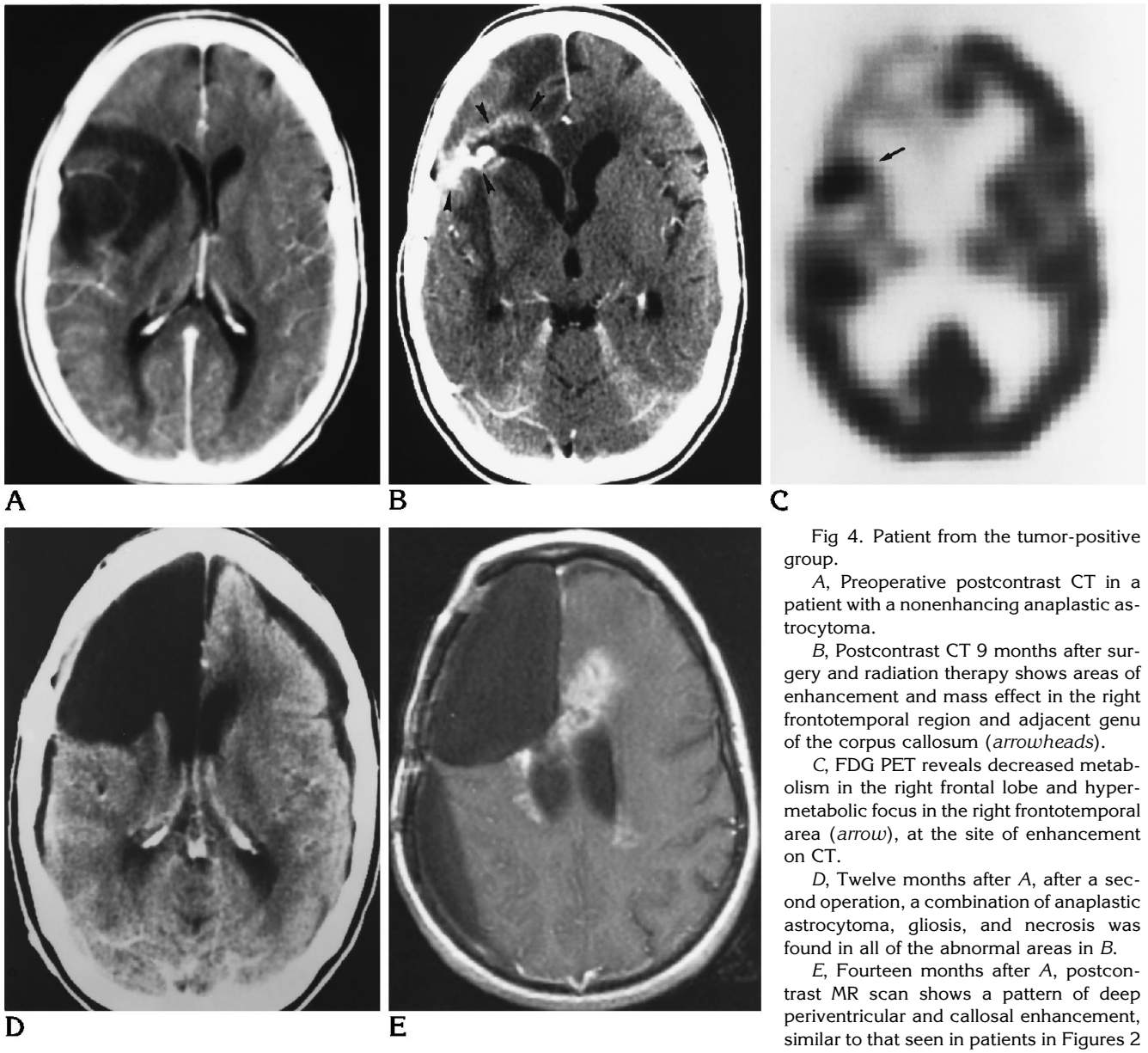

Fig 4. Patient from the tumor-positive group.

A, Preoperative postcontrast CT in a patient with a nonenhancing anaplastic astrocytoma.

B, Postcontrast CT 9 months after surgery and radiation therapy shows areas of enhancement and mass effect in the right frontotemporal region and adjacent genu of the corpus callosum (*arrowheads*).

C, FDG PET reveals decreased metabolism in the right frontal lobe and hypermetabolic focus in the right frontotemporal area (*arrow*), at the site of enhancement on CT.

D, Twelve months after *A*, after a second operation, a combination of anaplastic astrocytoma, gliosis, and necrosis was found in all of the abnormal areas in *B*.

E, Fourteen months after *A*, postcontrast MR scan shows a pattern of deep periventricular and callosal enhancement, similar to that seen in patients in Figures 2 and 3. Autopsy showed extensive necrosis throughout the brain. Possible infiltrating tumor cells were seen only along the inferior aspect of the surgical cavity.

all patients were inside the treatment portals. One patient had an additional contralateral lesion outside the portal; it was proved to be multicentric tumor. Seven of the 11 patients initially had solitary new lesions; follow-up scans later revealed additional lesions in 2 of these. Four of the 11 had more than one new lesion initially. In 4 patients the abnormalities were always heterogeneously enhancing; in 4 they were initially solid and later became ring enhancing, and in 3 patients the lesions remained solidly enhancing on multiple scans. Lesions were centered in the white matter in 8 patients and were corticomedullary in 3. Follow-up scans in 2 patients showed periventricular and callosal enhancement similar to that seen in the tumor-negative group. The initial dominant lesions in all 11 patients were at or within a few millimeters of the sites of treated tumors. The FDG PET scans in 2 patients revealed increased metabolic activity at the sites of the new lesions, proved to contain anaplastic astrocytomas in both. PET scanning near the time of the second operations was negative for hypermetabolic lesions in 3

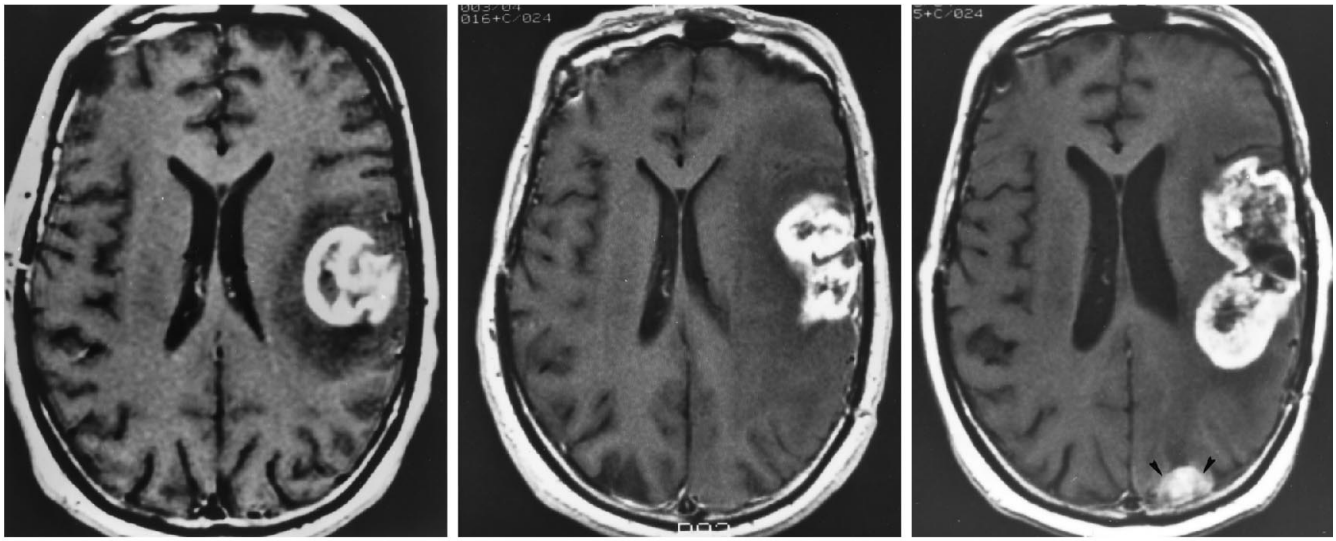

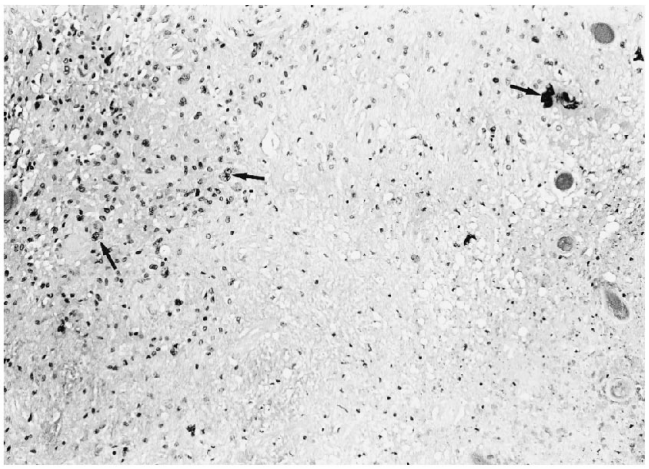

Fig 5. Patient in the tumor-positive group.

A, Preoperative postcontrast T1-weighted MR in a patient with glioblastoma multiforme.

B, Postoperative postcontrast scan 6 months after therapy shows abnormal enhancement within and around the surgical cavity. Surgery revealed tumor and necrotic brain.

C, Postcontrast scan 13 months after *A* shows a larger mass lesion with heterogeneous enhancement in the left parietal region. There is also a small left parietooccipital cortical and subcortical lesion (*arrowheads*). Autopsy revealed tumor and necrosis in the larger mass; the small lesion was predominantly neoplastic.

D, Histologic section from the larger mass, showing glioblastoma cells (*arrows*). Extensive necrosis is also present (*lower right*). Hematoxylin and eosin, original magnification × 125.

other patients in this group; the tissue from 1 patient was a low-grade mixed glioma, and low-grade astrocytomas were found in the other 2 patients.

One patient in this group underwent stereotactic biopsy; open resection of tissue was performed in the other 10. The tissue specimens in 9 of the 11 patients in this group demonstrated clear evidence of recurrent malignant glioma. In each patient there were also areas of necrosis, often felt to be caused by radiation effects apart from the presence of tumors because of the absence of high cellularity in the areas around the necrotic tissue. The pathologic diagnoses were more difficult in 2 other patients, whose tissues exhibited features of low-grade tumors and less anaplasia than seen in the original tumor specimen in each (possibly reflecting a beneficial effect from the radiation therapy).

Brains were available for autopsy in four patients in the tumor-positive group. In one patient, who had had a recurrent right frontal anaplastic astrocytoma, there was extensive necrosis of the periventricular white matter, the corpus callosum, and the fornix, presenting on MR imaging just before death as enhancing periventricular masses (Fig 4). Associated gliosis was present, but no convincing residual or recurrent tumor was seen in these areas. The appearance was similar to that of several patients in the tumor-negative group. The autopsy material from the other three patients showed definitive areas of tumor in each, and in one of these the tumor was multifocal (ipsilateral) (Fig 5). Two of these patients also had extensive

areas of radiation necrosis and gliosis, which was principally periventricular in one patient.

Discussion

It is well known that primary malignant tumors of the brain are essentially incurable and are resistant to most forms of therapy. Radiation therapy prolongs survival, especially with whole-brain radiation of 45 Gy and a tumor boost to 60 Gy (5). Use of the platinum-derivative drugs cisplatin or carboplatin combined with radiation therapy has been shown to potentiate the radiation effect (3, 4, 6). This occurrence may be attributable to increased sensitivity of hypoxic tumor cell DNA to radiation damage or by inhibition of repair of sublethal radiation damage. Carboplatin has considerable bone marrow toxicity. In the present study, delivering the radiation therapy in an accelerated fashion with three treatments daily permitted administration of carboplatin throughout the entire course of radiation before reaching bone marrow suppression. With accelerated fractionation radiation therapy, the overall treatment time is shortened by giving two or three doses daily, and the fraction size and total radiation dose are similar to those of conventional therapy (7). Accelerated fractionation radiation therapy has been used for rapidly proliferating tumors of the head and neck and brain. Studies have shown that, for brain tumors, an accelerated fractionation schedule is feasible, but that it does not seem to offer any improvement in long-term survival and may be associated with some reduction of quality of life after completing treatment (8, 9). However, it offers the advantage of an abbreviated treatment schedule in these patients, whose life expectancies are so short.

The late delayed form of cerebral radiation injury, which occurs a few months to many years after treatment, is the type of postradiation abnormality usually seen on imaging studies (10, 11). The term *radiation injury* includes a spectrum of pathologic changes from edema to necrosis, principally affecting the white matter. Focal and diffuse patterns of late delayed injury have been described and may occur independently or together (10). Tolerance of the brain to radiation therapy is related to the volume of brain irradiated, the total radiation dose, the size of the fraction, and the time interval between fractions, with the conventional time being 24 hours. The exact incidence of cerebral radiation necrosis is not known because of difficulties in obtaining surgical and postmortem correlations. Reported incidences of radiation necrosis after conventional therapy range between 5% and 24%, with higher figures found in autopsy subpopulations (12, 14). In our series, 9 of 81 patients (11%) had documented cerebral necrosis in the absence of definite associated tumors.

More is known of the pathologic correlate of focal radiation injury than the diffuse type, because the former patients are more often acutely ill, suspected clinically and by imaging studies to have recurrent tumors, and operated on. Histopathologic features of this lesion reflect small-vessel occlusion, white matter infarction, and necrosis. Typically seen are demyelination, reactive astrocytosis, fibrinous interstitial exudate, endothelial cell proliferation, fibrinoid necrosis and hyalinization of blood vessel walls, and coalescing areas of tissue necrosis with cavitation (10, 11, 15, 16). The endothelial and glial cell injuries permit leakage of contrast material into the interstitium. Surgical and autopsy material from the less frequently studied diffuse form of injury has revealed white matter pallor, demyelination, and reactive astrocytosis (15, 16). The margination of the abnormal area is sharp, oligodendrocytes are reduced, neurons are generally preserved, and vessel wall necrosis may be seen (16). Atypical large cells, probably astrocytes, are also frequently present, and these may be confused with tumor cells (15).

The irreversible and often progressive imaging abnormalities of the late delayed injury were originally described using CT, which showed focal or diffuse white matter hypodensity with or without associated contrast enhancement and mass effect (17, 20). Mikhael found that higher doses (60 to 70 Gy) correlated with the presence of parenchymal enhancement (17). Lee et al noted that the addition of chemotherapy, particularly intraarterial, to the radiation therapy regimen hastened the onset of CT abnormalities and also produced a greater incidence of clinical leukoencephalopathy (19). T2-weighted MR imaging displays the findings of radiation injury with much greater sensitivity than CT (10, 21–23). In the diffuse form, the abnormalities are usually symmetric when whole-brain radiation has been given and range from foci of hyperintense signal at the lateral ventricular angles to confluent signal abnormalities involving most of

the cerebral white matter. Such MR imaging abnormalities have been reported to occur in 38% to 100% of patients receiving cranial irradiation (10). More severe findings correlate with larger volumes of irradiated tissue, higher doses of radiation, increasing age, and a longer interval between radiation and imaging (12, 22). The milder forms may be difficult to distinguish from age-related deep–white matter ischemia on imaging studies (10). Enhancing white matter lesions have been reported with the use of gadopentetate dimeglumine, which may be of a "waxing-and-waning" nature and may eventually disappear (11). However, the frequency of enhancing brain lesions seen on MR imaging after conventional radiation therapy is not clearly established.

Focal radiation necrosis generally simulates a mass lesion and may develop several months to many years after treatment. These typically demonstrate a solitary ring-enhancing appearance on postcontrast CT and MR imaging and are centered in the white matter (10, 17, 20). Focal necrotic lesions tend to enlarge progressively, to exert mass effect, and often to require surgical intervention (10, 20). They may respond to steroid therapy (20). When a new ring-enhancing mass lesion develops in brain tissue included in the treatment portal for an extracranial malignancy or an intracranial arteriovenous malformation, the diagnosis of focal radiation necrosis of the brain is fairly straightforward. However, focal necrosis occurring after treatment of a malignant glioma is usually situated at or adjacent to the site of the treated tumor, and its appearance is essentially indistinguishable from that of recurrent tumor with the modalities of CT and MR. FDG PEToffers much more specificity between these two diseases. High-grade recurrent tumors demonstrate activity greater than that of normal cortical tissue, whereas areas of necrosis show much lower than normal activity (24–26). The distinction is not always perfect, however, because low-grade gliomas usually exhibit decreased metabolic activity and thus may be confused with radiation necrosis (25, 27, 28). Also, occasional recurrent malignant gliomas will demonstrate hypometabolism on FDG PET (27, 28). PET studies with the amino acid tracer L-methyl-carbon 11-methionine have shown a positive correlation between tumor grade and degree of radioisotope uptake and examples of increased uptake in lesions that were nonenhancing on CT studies (29, 30). Cerebral radiation necrosis showing activity similar to that of normal cortex has been observed on methyl-C-11-methionine PET imaging, and this technique has not been thought to be as accurate as FDG PET for differentiation between recurrent tumor and radiation necrosis (27). As no one modality is perfect for making this important distinction in the absence of tissue correlation, sometimes observation of the lesion over time and correlation with the clinical status will permit differentiation.

The MR scans of most patients in our series with proved necrosis but no definitive tumor demonstrated somewhat different patterns of abnormal contrast enhancement compared with previous descriptions of focal radiation necrosis. Most frequently seen were multiple enhancing peripheral lesions and striking multinodular or confluent enhancement around the lateral ventricles with or without an associated ring-enhancing mass at the site of treated tumor. This periventricular pattern resembled subependymal spread of the neoplasm. There has been one case report of nearly identical bilateral periventricular lesions mimicking a recurrent tumor seen on enhanced CT after radiation therapy for a frontal oligodendroglioma (31). Although the total radiation dose was 5200 Gy, the treatment was not really conventional, because the fraction size was nearly 350 cGy. The authors did not stress this fact and thought that the severe necrosis was related to the large postsurgical frontal cavity, permitting deposition of a higher dose at deeper levels of the brain. However, in our series, the patients illustrated in Figures 2 through 4 had smaller surgical cavities than the other reported patient at the time of radiation therapy administration but developed the same periventricular lesions. We found no apparent correlation between the size of the postoperative cavity and the severity or extent of enhancing lesions.

The occurrence of necrotic lesions at the lateral margins of the ventricles may be explained by the fact that this is the terminal zone of the blood supply of the long medullary arteries arising from leptomeningeal arteries. This region would be the most vulnerable portion of this vascular distribution to ischemic effects produced by postradiation vasculopathy. The previous theory of a deep watershed zone about 1 cm from the ventricular margins seems to have been disproved by several investigators (32,

33). The frequent presence of enhancing lesions in the corpus callosum and at corticomedullary junctions is more difficult to understand. Moody et al have shown that these regions, with the exception of the splenium of the corpus callosum, are well protected from ischemia by a blood supply consisting of short penetrating arterioles (32). Perhaps the presence of lesions in these locations indicates severe combined toxicity of accelerated fractionation radiation and simultaneous carboplatin infusion to small arteries and arterioles.

The FDG PET findings in the two groups of patients are largely consistent with previously reported findings using this modality for recurrent tumor and radiation necrosis of the brain (24, 26, 28). PET results in four of five cases in the tumor-negative group were negative for hypermetabolic foci. There was an unexpected finding of a hypermetabolic focus in one patient in this group, which at autopsy was shown not to contain tumor cells. The same discrepant FDG PET and histologic result has also been seen in two other patients from this treatment protocol who are not a part of this report, and the need for caution in interpreting FDG PET scans in patients with malignant gliomas who have undergone intensive radiation therapy has been emphasized (34). Three patients in the tumor-positive group with only low-grade gliomas identified histologically at the time of posttreatment PET scanning showed no areas of abnormally increased isotope uptake, exemplifying the caveat mentioned above for FDG PET in low-grade gliomas. PET results were positive in two other patients in this group, correlating with the presence of anaplastic tumor.

In summary, we report preliminary imaging findings of patients treated with accelerated fractionation radiation therapy in combination with the radiation-sensitizing chemotherapeutic agent carboplatin. We found an 11% incidence of radiation necrosis of the brain in the absence of definitive associated tumors. The imaging appearance of these radiation necrosis lesions differed somewhat from previously described focal lesions after conventional therapy in that they were typically multiple and tended to affect the central regions of the brain, that is, the corpus callosum and the immediate periventricular white matter. Lesions in these locations may mimic recurrent tumors but were observed to develop more slowly than relapsing tumors and were often found at a significant distance from the original tumor sites. The increased sensitivity of contrast-enhanced MR imaging over enhanced CT most probably enabled recognition of many of these lesions when they were small. Most MR imaging reports of radiation injury to the brain have been before the availability of paramagnetic contrast material. To ascertain how much more injurious accelerated fractionation radiation and carboplatin therapy may be to the brain than conventional therapy, it would be helpful to have a gadolinium-enhanced MR series of patients treated with conventional radiation therapy for comparison with our results. Analysis of the data from our series of patients is in progress to determine whether this mode of therapy results in improved survival compared with conventional treatment.

References

1. Kyritsis AP, Saya H, Levin VA. Molecular pathogenesis and management of gliomas. *Neuroimaging Clin North Am* 1993;3: 735–744
2. Andersen AP. Postoperative irradiation of glioblastomas: results in a randomized series. *Acta Radiol Oncol* 1978;17:475–484
3. Douple EB, Richmond RC, OHara JA, Coughlin CT. Carboplatin as a potentiator of radiation therapy. *Cancer Treat Rev* 1985;12: 111–124
4. Nias AH. Radiation and platinum drug interaction. *Int J Radiat Biol* 1985;48:297–314
5. Shapiro WR. Therapy of adult malignant brain tumors: what have the clinical trials taught us? *Semin Oncol* 1986;13:38–45
6. Fu KK, Rayner PA, Lam KN. Modification of the effects of continuous low dose rate irradiation by concurrent chemotherapy infusion. *Int J Radiat Oncol Biol Phys* 1984;10:1473–1478
7. Thames HD, Peters LJ, Withers HR, Fletcher GH. Accelerated fractination vs hyperfractination: rationales for several treatments per day. *Int J Radiat Oncol Biol Phys* 1983;9:127–138
8. Keim H, Potthoff K, Schmidt K, Schiebusch M, Neiss A, Trott KR. Survival and quality of life after continuous accelerated radiotherapy of glioblastoma. *Radiother Oncol* 1987;9:21–26
9. Horiot JC, van den Bogaert W, Ang KK, et al. European organization for research on treatment of cancer trials using radiotherapy with multiple fractions per day: a 1978–1987 survey. *Front Radiat Ther Oncol* 1988;22:149–161
10. Valk PE, Dillon WP. Radiation injury of the brain. *AJNR Am J Neuroradiol* 1991;12:45–62
11. Ball WS, Prenger EC, Ballard ET. Neurotoxicity of radio/chemotherapy in children: pathologic and MR correlation. *AJNR Am J Neuroradiol* 1992;13:761–776
12. Marks JE, Baglan RJ, Prassad SC, Blank WF. Cerebral radionecrosis: incidence and risk in relation to dose, time, fractionation and volume. *Int J Radiat Oncol Biol Phys* 1981;7:243–252
13. Marsa GW, Goffinet DR, Rubenstein LJ, Bagshaw MA. Megavoltage irradiation in the treatment of gliomas of the brain and spinal cord. *Cancer* 1975;36:1681–1689
14. Burger PC, Mahaley MS, Dudka L, Vogel FS. The morphologic effects of radiation administered therapeutically for intracranial gliomas: a postmortem study of 25 cases. *Cancer* 1979;44: 1256–1272

15. Burger PC, Boyko OB. The pathology of central nervous system radiation injury. In: Gutin Ph, Leibel SA, Sheline GE, eds. *Radiation Injury to the Nervous System*. New York: Raven Press; 1991: 191–208
16. De Reuck J, Vander Eecken H. The anatomy of the late radiation encephalopathy. *Eur Neurol* 1975;13:481–494
17. Mikhael MA. Radiation necrosis of the brain: correlation between patterns on computed tomography and dose of radiation. *J Comput Assist Tomogr* 1979;3:241–249
18. Kingsley DPE, Kendall BE. CT of the adverse effects of therapeutic radiation of the central nervous system. *AJNR Am J Neuroradiol* 1981;2:453–460
19. Lee Y-Y, Nauert C, Glass JP. Treatment-related white matter changes in cancer patients. *Cancer* 1986;57:1473–1482
20. Glass JP, Hwang T-L, Leavens ME, Libshitz HI. Cerebral radiation necrosis following treatment of extracranial malignancies. *Cancer* 1984;54:1966–1972
21. Curnes JT, Laster DW, Ball MR, Moody DM, Witcofski RL. MRI of radiation injury to the brain. *AJNR Am J Neuroradiol* 1986;7: 389–394
22. Constine LS, Konski A, Ekholm S, McDonald S, Rubin P. Adverse effects of brain irradiation correlated with MR and CT imaging. *Int J Radiat Oncol Biol Phys* 1988;15:319–330
23. Tsuruda JS, Kortman KE, Bradley WG, Wheeler DC, Van Dalsem W, Bradley TP. Radiation effects on cerebral white matter: MR evaluation. *AJNR Am J Neuroradiol* 1987;8:431–437
24. Patronas NJ, Di Chiro G, Brooks RA, et al. Work in progress: [^{18}F]fluorodeoxyglucose and positron emission tomography in the evaluation of radiation necrosis of the brain. *Radiology* 1982;144: 885–889
25. De Chiro G, Oldfield E, Wright DC. Cerebral necrosis after radiotherapy and/or intraarterial chemotherapy for brain tumors: PET and neuropathologic studies. *AJNR Am J Neuroradiol* 1987;8: 1083–1091
26. Di Chiro G, Brooks RA, Bairamian D, et al. Diagnostic and prognostic value of positron emission tomography using [^{18}F]fluorodeoxyglucose in brain tumors. In: Reivich M, Alavi A, eds. *Positron Emission Tomography*. New York: Alan R. Liss, 1985:291–309
27. Ogawa T, Kanno I, Shishido F, et al. Clinical value of PET with ^{18}F-fluorodeoxyglucose and L-methyl-^{11}C-methionine for diagnosis of recurrent brain tumor and radiation injury. *Acta Radiol* 1991;32:197–202
28. Valk PE, Budinger TF, Levin VA, Silver P, Gutin PH, Doyle WK. PET of malignant cerebral tumors after interstitial brachytherapy: demonstration of metabolic activity and correlation with clinical outcome. *J Neurosurg* 1988;69:830–838
29. Lilja A, Bergstrom K, Hartvig P, et al. Dynamic study of supratentorial gliomas with L-methyl-^{11}C-methionine and positron emission tomography. *AJNR Am J Neuroradiol* 1985;6:505–514
30. Derlon J-M, Bourdet C, Bustany P, et al. [^{11}C] L-methionine uptake in gliomas. *Neurosurgery* 1989;25:720–728
31. Safdari H, Boluix B, Gros C. Multifocal brain radionecrosis masquerading as tumor dissemination. *Surg Neurol* 1984;21:35–41
32. Moody DM, Bell MA, Challa VR. Features of the cerebral vascular pattern that predict vulnerability to perfusion or oxygenation deficiency: an anatomic study. *AJNR Am J Neuroradiol* 1990;11: 431–439
33. Nelson MD, Gonzalez-Gomez I, Gilles FH. The search for human telencephalic ventriculofugal arteries. *AJNR Am J Neuroradiol* 1991;12:215–222
34. Janus TJ, Kim EE, Tilbury R, Bruner JM, Yung WKA. Use of [^{18}F]fluorodeoxyglucose positron emission tomography in patients with primary malignant brain tumors. *Ann Neurol* 1993;33: 540–548